

Action of Zirconium Phosphate as a Catalyst for the Oxydehydrogenation of Ethylbenzene to Styrene

G. EMIG AND H. HOFMANN

Institut für Technische Chemie I, Egerlandstrasse 3, D-8520 Erlangen, Germany

Received September 7, 1982; revised May 10, 1983

Zirconium phosphate was shown to be suitable because of its texture and temperature-resistance as a catalyst carrier in the oxydehydrogenation of ethylbenzene to styrene, but that it is not acting itself as the catalyst. During the reaction an organic polymer with groups containing oxygen, formed by way of the reaction product styrene, is precipitated on the catalyst carrier and acts as the actual dehydrogenation catalyst. Because of steady state conditions between the continuous formation of this activated coke and the burning-off of the coke, the catalyst system retains a constant level of activity over a long period of time, but can also be regenerated at will, if need be, by total oxidation of the coke. The redox effect of activated coke can be augmented, as expected, by halogens. The pore structure of the crystalline zirconium phosphate (produced according to specific manufacturing procedures) appears to be particularly suitable for this reaction in the sense that it is a selective catalyst.

INTRODUCTION

The oxydehydrogenation of saturated hydrocarbons is currently of increasing importance, both because of energetic and thermodynamic reasons. In contrast to the classical styrene production by catalytic dehydrogenation at 850 to 950 K, the oxydehydrogenation can be performed at 650 to 750 K with a higher degree of conversion and much lower steam content in the reaction mixture.

The catalysts which have been described in the literature up to now for the oxydehydrogenation of ethylbenzene (EB) to styrene together with their operating conditions are listed in Table 1. For the most part, they consist of metallic oxides, phosphates, and organic polymers extending as far as activated carbon (1-17, 30). For these catalysts the selectivity achieved is dependent upon the conversion as well as the molar ratio of oxygen to ethylbenzene. In many publications a redox reaction has been assumed as a possible mechanism for oxydehydrogenation (17, 18).

The conversion and selectivity as a func-

tion of temperature for six suitable catalysts, either commercially available or produced according to given references, is shown in Fig. 1. The results refer to 6-8 h of operation.

Zirconium phosphate (ZrP) appeared to be the most promising system and was thus subjected to a more thorough investigation in an isothermal microintegral reactor in order to test whether the values given in Fig. 1 could still be attained after a longer period of operation. Figure 2 shows a typical result for up to 235 h on stream. Details concerning the conversion and selectivity behavior in the first 16 h on stream are shown in Fig. 3.

Particularly striking are the values for conversion and selectivity which both increase from a small initial value to reach a maximum within the first hours of operation and then slowly decrease with time on stream.

In a previous paper (25) we reported details of the experimental equipment, together with the kinetics using the ZrP catalyst and some speculations about its industrial application. In the present study,

TABLE 1
Literature Survey of Catalyst Systems for the Oxydehydrogenation of Ethylbenzene (EB)
with Operating Data

No.	Year of publication	Catalyst system	Specific surface area (m ² /g)	T (°C)	EB/O ₂	EB/Inert	Residence time W/F (g cat/g EB/h)	Conversion U (%)	Selectivity S (%)	Ref.
1	1965	Sb ₂ O ₃	—	450	1/1	1/5.7	2.8	51	87	(1)
2	1968	Sb ₂ O ₃	10–300	430–500	1/0.2–0.5	1/3	Fluidized bed	42	90	(2)
3	1968	Fe ₂ O ₃	—	560–680	1/0.04–0.32	1/5–10	Multistage reactor	50–70	90	(3)
4	1970	Fe ₂ O ₃	—	—	—	—	—	—	—	(4)
5	1972	Al ₂ O ₃	180	450	1/1.2	1/4.8	2.5	59	79	(5)
6	1973	ZnCrFeO ₄	—	425	1/0.33	—	—	17	86	(6)
7	1973	Ce/Zr-P	—	572	1/1	1/8	2.3	68	86	(7)
8	1973	PNC	—	200	1/	1/	—	2	100	(8)
9	1974	Ni/W-oxide on Al ₂ O ₃	3.2	460	1/1	1/8	18.8	40	77	(9)
10	1974	Co/Mo	—	450	1/0.8	—	—	40	83	(10)
11	1976	Earth alkaline-Ni-P	—	535	1/0.78	1/5.26	6.69	69	87	(11)
12	1978	Active carbon	6.24–955	400	—	—	Pulse reactor	—	—	(12)
13	1978	Al ₂ O ₃	—	450	1/1	—	Pulse reactor	—	—	(13)
14	1979	Zr-phosphate	7	450	1/1.24	1/3.67	0.9	27	90	(14)
15	1979	PPAN	19	325	1/43	1/163	260.6	≅80	≅100	(15)
16	1981	Al ₂ O ₃	—	500	1/0.92	1/3.48	Space velocity 3333 h ⁻¹ (pulse reactor)	9–77	64–88	(16)
17	1981	SnO ₂ -P ₂ O ₅	5.9–13.1	450	1/1–1/0.5	—	0.017–0.325	10–20	80–90	(17)

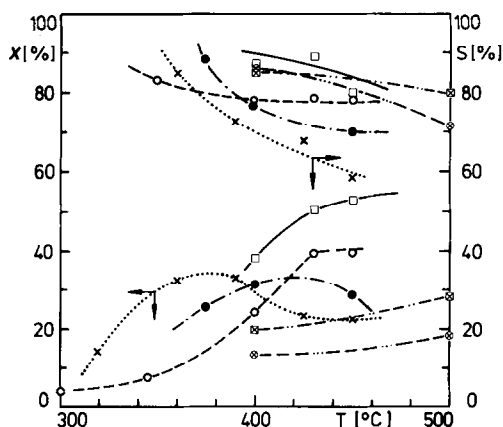


FIG. 1. Conversion and selectivity (after approx. 6–8 h on stream) as a function of temperature for different catalysts

Type	Catalyst	Modified residence time (W/F)	EB/O ₂ /N ₂
● Grace SP2 1781/82	Al ₂ O ₃ /SiO ₂	3.14	1/1/7
○ Harshaw A1-0104 T	γ-Al ₂ O ₃	3.14	1/1/7
× Bergbauforschung AKE	Active carbon	1.88	1/1/7
□ Ger. Pat. 3114350	ZrP-1	3.5	1/1/7
⊗ US Pat. 3935126	CaNiP	3.0	1/1/6
⊠ According to (9)	W/Ni	3.4	1/1/8

further investigations and results are described to clarify the unusual activity vs time-on-stream behavior.

EXPERIMENTAL

Most of the experiments have been performed in an isothermal microintegral reactor (19) (length of the catalyst packing 120 mm, diameter 12 mm, particle diameter 1 mm) operated at normal pressure. The carbon deposit of the catalyst was determined by removing the catalyst from the reactor, burning off the carbon and quantitatively determining the amounts of CO/CO₂. The carbon deposit as a function of time on stream has been studied in investigations in a DTG setup (Netsch) and scanning electron photomicrographs of the catalyst have been made. The investigation of the BET surface according to DIN 66131 as well as pore volume distribution (27) has been performed by N₂ low-temperature adsorption measurements (Orr-analyzer, Microme-

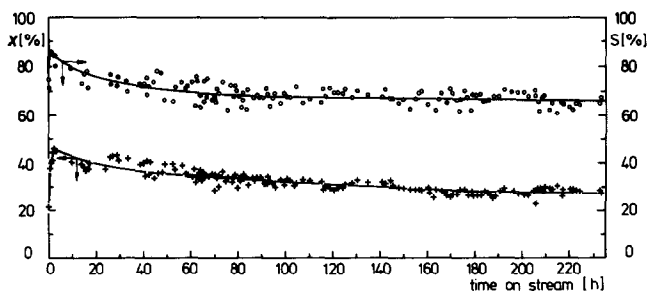


FIG. 2. Conversion and selectivity of active ZrP as a function of time on stream ($T = 450^{\circ}\text{C}$; $W/F = 3.14 \text{ g catalyst} \cdot \text{h/g EB}$; $\text{EB}/\text{O}_2/\text{N}_2 = 1/1/7$).

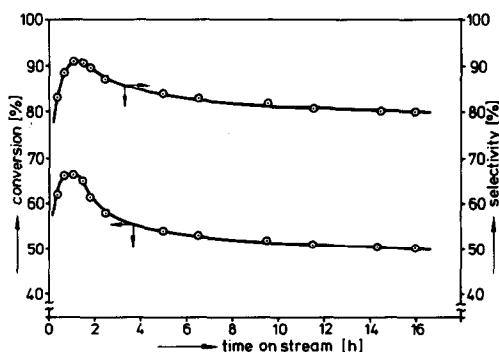


FIG. 3. Conversion and selectivity behavior of an active ZrP catalyst during the first hours of time on stream. $\text{EB}/\text{N}_2 = 1/7$, $\text{EB}/\text{O}_2 = 1/1$. $W/F = 3.14 \text{ g catal.} \cdot \text{h/g EB}$ $T = 450^{\circ}\text{C}$.

ritics). Mechanistic studies of the catalyst behavior in the first period of time on stream and with different reaction mixtures

have been additionally performed in a pulse reactor (26). The acidity of the catalyst has been investigated first by titration with *n*-butylamine and Hammett indicators (28) and secondly by TPD of pyridine in the DTG equipment.

RESULTS AND DISCUSSION

The conversion and selectivity characteristics given in Figs. 2 and 3 were reproducible for up to 30 regenerations (with a hot O_2/N_2 mixture) over a total operating period of 3500 h on stream. After a short exposure to the reaction mixture the catalyst turned from white into black suggesting a carbon deposit. This was confirmed by a quantitative determination of carbon content, depicted simultaneously with the BET surface area as a function of time on stream

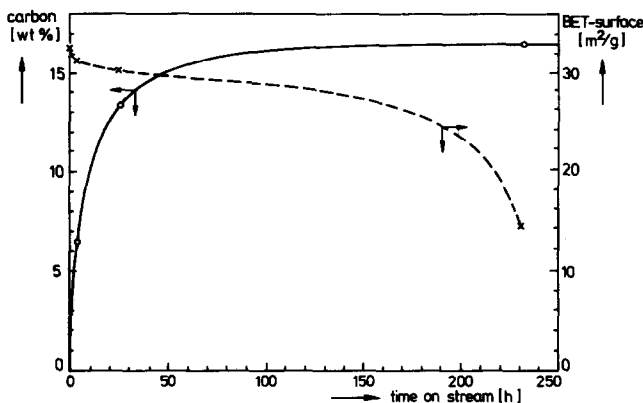


FIG. 4. Carbon content and BET surface of active ZrP catalyst as a function of time on stream (operating conditions same as in Fig. 2).

TABLE 2
Conversion (X) and Selectivity (S) for Different ZrP Catalyst Samples

W/F (g cat · h/g EB)	EB/N ₂ (mol/mol)	EB/O ₂ (mol/mol)	T (°C)	ZrP-1		ZrP-2		ZrP-3	
				X(%)	S(%)	X(%)	S(%)	X(%)	S(%)
3.14	1/10	1/1	450	51.8	78.6	18.1	77.0	55.0	86.1
1.88	1/7	1/0.7	450	39.2	73.0	16.3	76.2	40.6	89.1
0.9	1/7	1/1	450	39.8	86.1	9.5	82.1	37.0	89.1

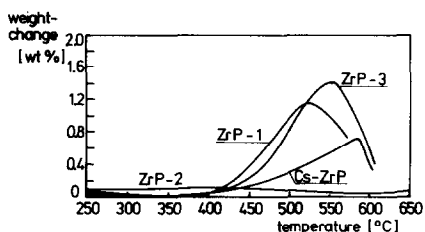


FIG. 5. Weight change of different ZrP catalysts as a function of temperature from DTG measurements.

in Fig. 4. The asymptotic level of carbon on the catalyst was heavily dependent on the ratio of ethylbenzene to oxygen in the feeds; the greater the oxygen content, the lower the carbon content on the catalyst (19).

The question now arises as to why the activity of the catalyst does not decline despite the high carbon content (see Fig. 4)

and as to how the catalytic effect can be explained. Figure 5 exhibits investigations in a DTG setup with increasing temperature (0.5 K min^{-1}) for four catalyst samples of different manufacture with ethylbenzene / O₂/N₂ as the reaction mixture. A clear increase in the weight near the most favorable operating temperatures of 400–550°C can only be found in the active catalysts (ZrP-1, ZrP-3, and Cs-ZrP), whereas a less active sample (ZrP-2) shows practically no change in weight. This latter catalyst has been prepared according to a slightly different preparation procedure, leading to lower conversion (see Table 2).

It can be concluded from the color of the catalysts and the CO measurements in the exit gas that the increase in weight must be caused by the carbon content. One can tell that active and inactive catalysts are differ-

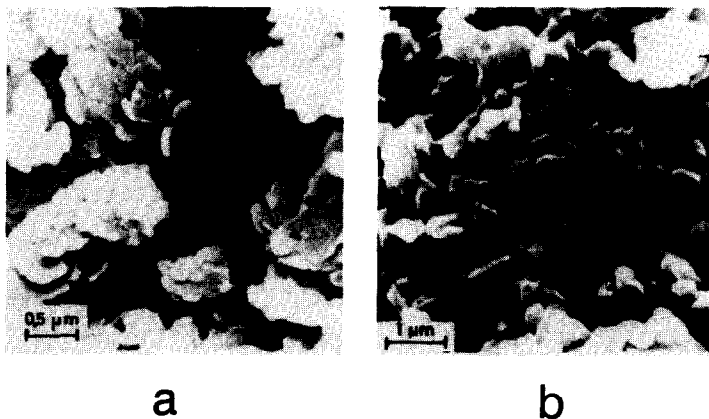


FIG. 6. Electron photomicrographs of fresh ZrP catalysts. (a) High activity ZrP-1; (b) low activity ZrP-2.

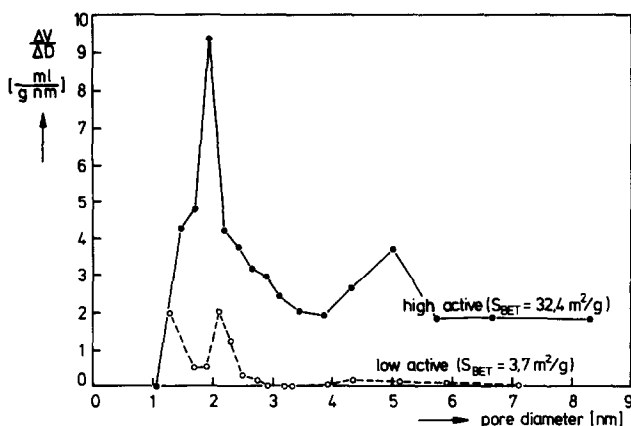


FIG. 7. BET surface area and pore volume distribution for high active (ZrP-1) and low active (ZrP-2) freshly prepared ZrP catalyst.

ent simply by looking at their scanning electron photomicrographs (Fig. 6). The active catalyst exhibits a very obvious crystalline platy structure, whereas the less active catalyst has a more amorphous, "smeared" appearance.

Differences can also be found in the texture of the catalysts, characterized by their surface and pore volume distribution (cf. Fig. 7). Apart from the fact that its surface is 10 times as large, the active catalyst has a clear pore diameter maximum around 2 nm. Obviously the texture of the catalyst also has an influence on the catalytic activity. The change in the pore structure along with

the increasing precipitation of carbon on the catalyst is shown in Fig. 8. With increasing time on stream, one sees a slight shifting of the maximum to smaller pore radii and a decrease in the number of larger pores; however, even after a relatively long period of operation, there are still quite a large number of pores in the range 1–3 nm (the BET surface areas which correspond to the different times on stream can be seen in Fig. 4).

In order to decide whether or not acid centers of the ZrP are significant for the catalytic mechanism, the ZrP system which is present at reaction temperatures as or-

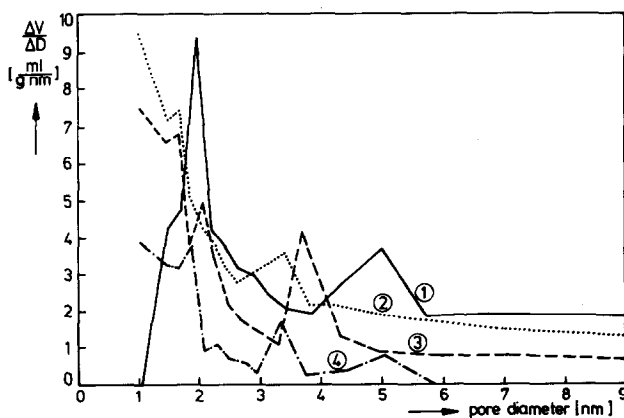


FIG. 8. Change of catalyst texture with time on stream for an active ZrP catalyst. ① Fresh catalyst. ② After 3 h on stream. ③ After 25 h on stream. ④ After 233 h on stream.

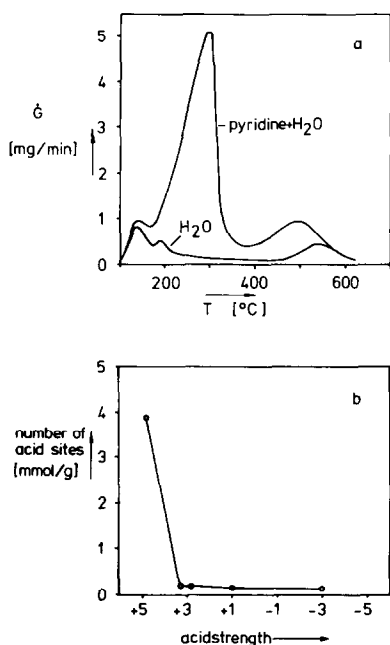


FIG. 9. TPD spectrum (a) and number of sites (b) for ZrP-1 catalysts.

thophosphate $\text{Zr}(\text{HPO}_4)_2$ and exhibits a few millimoles per gram of acid centers of various strengths (see Fig. 9) was converted to diphosphate ZrP_2O_7 by heating the original

catalyst to a temperature of 1100°C , after which no more acid centers were evident. However, in respect to activity and selectivity, this diphosphate exhibits a reaction behavior comparable to the normal ZrP catalyst shown in Fig. 2 and 3, i.e., acid centers of ZrP are apparently not significant for the catalytic mechanism.

On the other hand, diphosphate (see Curve 2 in Fig. 10) has similar pore structure (with a maximum between 1 and 3 nm and exhibits a shift to smaller pore radii after a longer time on stream as shown in Fig. 10 by Curve 3 and a BET surface area ($22.4 \text{ m}^2/\text{g}$) comparable with ZrP-1 (cf. Fig. 7) which means that the physical structure seems to be responsible for activity and selectivity.

To clarify the chemical nature of the "carbon precipitation" on the catalyst, a quantitative organic C/H/O analysis was carried out for the orthophosphate (dependent upon the length of time on stream) as well as for the diphosphate (after 16 hours on stream). Table 3 lists these results together with values for an Al_2O_3 catalyst as well as the theoretical C/H/O values for polynaphthoquinone. Mainly the results

TABLE 3
Chemical Composition of Coke Deposits

Experiment	Coke content (wt%)	Composition (wt%)			Empirical formula	C/H ratio
		C	H	O		
ZrP (3 h)	6.5	55.7	8.9	35.4	$\text{C}_{2.1}\text{H}_4\text{O}$	0.52
ZrP (25 h)	13.3	64.4	6.5	29.1	$\text{C}_{2.9}\text{H}_{3.6}\text{O}$	0.82
ZrP (233 h)	16.4	70.1	5.1	24.8	$\text{C}_{3.8}\text{H}_{3.3}\text{O}$	1.14
ZrP_2O_7 (16 h)	3.9	87.4	2.6	10.0	$\text{C}_{11.7}\text{H}_{4.2}\text{O}$	2.79
Al_2O_3 (16)	2.1–25.0	76.7–82.0	12.4–2.4	10.9–15.6	$\text{C}_{9.4}\text{H}_{18.2}\text{O}-\text{C}_{7.0}\text{H}_{2.5}\text{O}$	0.52– 2.80
Polynaphtho- quinone (8)	100	76.9	2.6	20.5	$\text{C}_{5.0}\text{H}_{2.0}\text{O}$	2.5

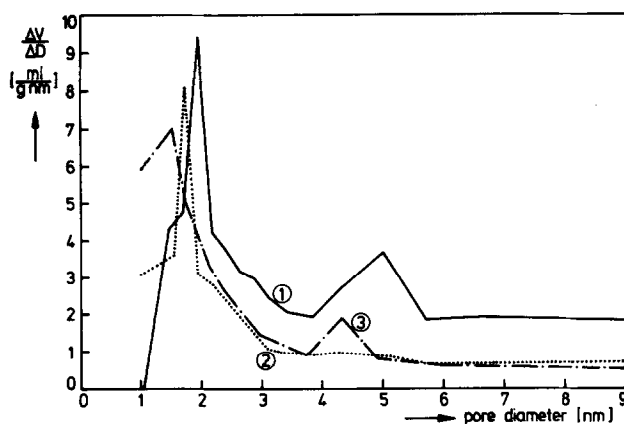


FIG. 10. Comparison of catalyst texture of orthophosphate (①, fresh) and diphosphate (②, fresh and ③, after 16 h of time on stream).

with diphosphate suggest as a hypothesis that the partially oxidized carbon precipitate can be characterized (see Fig. 14) as a substance similar to polynaphthoquinone (from now on abbreviated as coke) and the catalytic activity is due to an organic redox system with quinoid groups. This suggestion is supported by ESR measurements of fresh ZrP as well as coke-loaded ZrP catalyst. The fresh carrier showed no ESR signal, whereas the coke-loaded ZrP showed signals with a g value of 2.0032 which according to the dependence of the g values on oxygen content for selected coals (see (23)) corresponds to an oxygen content in the range of 5–10 wt%.

It has been known for some time that by treating activated carbon with oxygen, quinoid groups can be formed along with other surface oxides (21, 22) which in turn produce oxidative reactions in the gaseous reactant mixture even in the absence of oxygen (e.g., during the oxidation of SO_2 to SO_3).

Therefore ZrP acts mainly as a carrier (with a suitable texture) which would also explain why there is only a small degree of initial activity found in the pulse experiment shown in Fig. 12. If this hypothesis is correct, the catalytic effect must essentially be independent of the chemical nature of the carrier material and this is, in fact, the

case, as demonstrated in Fig. 1. Differences in activity and selectivity such as are shown in Table 2 should have their origin mainly in the texture of the carrier material. The properties of the different catalysts used in this study are given in Table 4.

The above characteristics are even more clearly seen in Fig. 11, where the activity and selectivity for styrene production as a function of time on stream is shown for a typical cracking catalyst (Grace SP2 1781/1782). During the first 3 h on stream, in which hardly any coke is precipitated, only the formation of the cracking products of ethylbenzene could be observed, i.e., the formation of benzene and toluene; styrene formation took place only after 3 h, at the same time as coke was increasingly precipitated on the surface. The cracking of ethylbenzene ceased at the same time (benzene

TABLE 4

Properties of Catalyst Used in This Study

Catalyst	Specific surface (m ² /g)	Pore volume (ml/g)	Porosity	Maximum of pore radius (nm)
Al ₂ O ₃ /SiO ₂	375	0.4	—	—
γ-Al ₂ O ₃	100	0.36	0.56	Bimodal 10,80
Active carbon	1280	—	—	1
ZrP-1	36.9	0.34	0.46	2

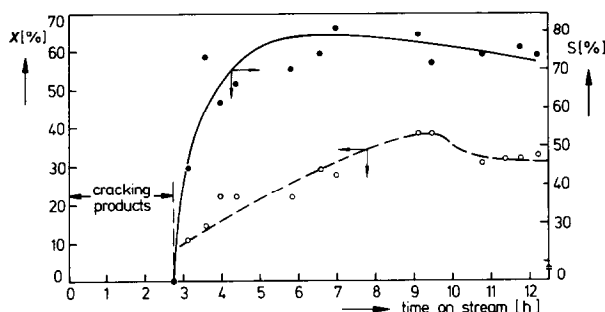


FIG. 11. Conversion and selectivity as function of time on stream for a typical cracking catalyst ($T = 400^{\circ}\text{C}$; $W/F = 3.14$; $\text{EB}/\text{O}_2/\text{N}_2 = 1/1/7$).

and toluene were no longer produced), apparently because the acid centers necessary for cracking were "covered up" by coke deposits.

It is appropriate now to discuss the results presented so far. The following conclusions can be drawn from these experimental results:

(1) In the stationary phase of operation, the coke on the catalyst surface is the real catalytically active component. It was also not very likely that zirconium phosphate would be involved in a redox mechanism, because zirconium oxide, like aluminum oxide, is very resistant to reduction or oxidation, in marked contrast to vanadium oxide and molybdenum oxide.

(2) An important requirement for the activity of the catalyst is a suitable texture with pores of about 2 nm diameter and a sufficiently large BET surface in the range of $30 \text{ m}^2/\text{g}$, as supplied by zirconium phosphate of suitable preparation.

(3) Acid centers, such as those on zirconium phosphate, are not significant for oxydehydrogenation, because they are covered with coke during the steady state phase of the reaction; nevertheless, they can accelerate the precipitation of coke onto the surface (cf. coke formation on acid cracking catalysts in the presence of aromatic hydrocarbons) which has also been demonstrated for the formation of activated coke on Al_2O_3 (16).

(4) The activity and selectivity vs time behavior (cf. Figs. 3 and 11) is nearly independent of the chemical nature of the catalyst carrier. Three phases are involved: there is a rise phase (sometimes after a time lag), a maximum phase, and a steady state phase. Coke formation begins in the rise phase and produces a monomolecular coating at a coke content of about 3–6%. At the maximum the entire inner surface of ZrP (coated with an active layer of coke) is available for the main reaction and there are very few side reactions to CO_x . In the steady state phase, a certain number of the pores are apparently not accessible for the rather large ethylbenzene molecule (molecular dimension ca. 0.7 nm) because of the continued formation of coke. However, the smaller oxygen molecule (0.12 nm) still has access as before (cf. separation of iso- and n-hydrocarbons, where the differences in the molecular dimensions are even smaller) and it continues to oxidize the coke to CO_x until ethylbenzene again has access to the partially oxidized surface.

(5) On the average only a part of the total surface is available for the main reaction in the steady state phase and the percentage of the side reaction is larger (decrease in selectivity) as compared to the maximum. Without this steady state between carbonization and the burning-off of coke (whose quantity depends, of course, upon the reaction temperature and the oxygen content of

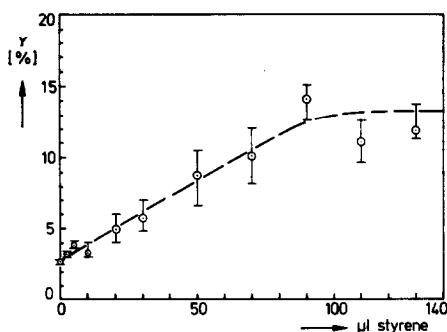


FIG. 12. Yield of styrene as a function of the formation of active coke (range indicated corresponds to highest and lowest individual results); temperature 435°C, carrier gas flow rate of 24 ml NTP/min.

the reaction mixture) the constant activity and selectivity over a long period of time could not be explained.

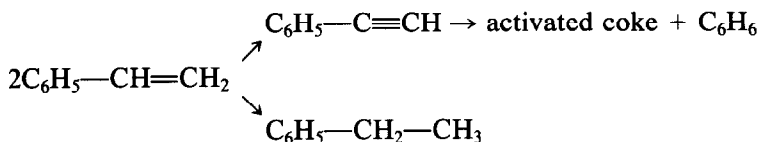
(6) The carbonization process, along with the zeolite-like structure of zirconium phosphate (29), could also explain the fact that only CO_x appears as a side product. Ethylbenzene is very selectively converted on the coke to styrene which in turn can be easily polymerized at higher temperatures. Because of its molecular size, this polymer can then leave the pore system only as CO_x .

(7) If a quinoid redox system is assumed, then it should preferentially originate from styrene. In order to clarify this point, experiments to determine the formation of activated coke were carried out in the pulse

reactor, starting with ethylbenzene on the one hand and styrene on the other. In the first experiment, 200 pulses of 0.5 μl ethylbenzene, with N_2 as the carrier gas, were injected on a fresh ZrP-1 catalyst at 435°C. After every 40 pulses, 500 μl of oxygen were injected (i.e., total molar ratio of EB : O_2 of about 1 : 1). Over the entire duration of the experiment, the degree of formation of styrene remained at about 3–5%, which in essence probably indicates an initial dehydrogenation activity of the fresh catalyst. The originally white catalyst turned merely to a slight and irregular light-grey color, in comparison to the coated, anthracite-colored activated catalyst.

In contrast, when pulses of styrene alternating with oxygen were injected, instead of ethylbenzene alternating with oxygen (under otherwise equal conditions) the styrene yield and selectivity continued to increase if an ethylbenzene pulse was interspersed to test the actual activity of the catalyst (experimental points of Fig. 12), finally attaining values reached in an integral reactor operating under steady state conditions.

Figure 13 shows, in addition, how the styrene pulses are partially converted by the uncoated ZrP to ethylbenzene and benzene in the above-mentioned initial phase; this could perhaps be explained by the following reaction scheme:



Alternatively benzene could be formed by cracking of styrene or ethylbenzene and ethylbenzene could be formed by hydrogen transfer during styrene condensation as proposed in Fig. 14.

(8) Parallel experiments with butene as a starting material showed that aliphatics apparently cannot form "activated coke" in

the same way.

(9) If the styrene formation proceeds according to a redox mechanism, one can formulate a reaction cycle with an organic redox system analogous to the reaction cycles with inorganic redox systems (18); in this organic redox system the quinoid groups would first be formed during the re-

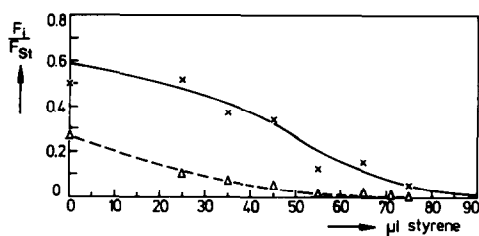


FIG. 13. Relative ethylbenzene- and benzene-peak versus amount of styrene pulsed (\times , ethylbenzene; Δ , benzene); temperature 435°C , carrier gas flow rate 24 ml NTP/min.

action (Fig. 14). In this case, the entire reaction must be able to be divided into the partial steps of hydrogen abstraction (with

reduction of the coke surface) and coke reoxidation in the presence of oxygen (re-activation of the activated coke) to form H_2O .

Experiments in a pulse reactor with pure ethylbenzene (in the absence of oxygen) and with about 1 g of activated (oxidized) catalyst show the expected decrease, as hypothesized, in the degree of formation of styrene which in turn depends upon the amount (proportional to the number of pulses) of styrene formed (Fig. 15). If one linearly extrapolates this process to a degree of formation of zero (intersection with the abscissa axis), this then corresponds to approximately a total of $220 \mu\text{mol}$ of

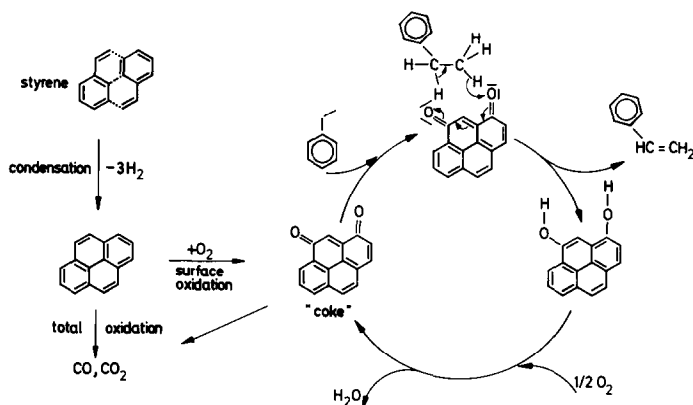


FIG. 14. Speculative mechanism for the oxydehydrogenation of ethylbenzene to styrene.

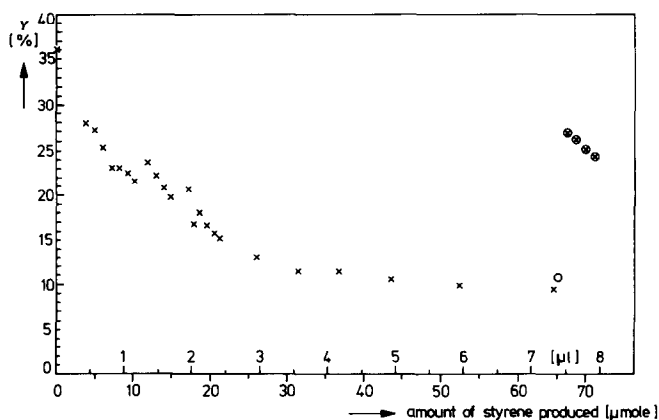


FIG. 15. Yield of styrene per pulse versus amount of styrene produced ($T = 435^{\circ}\text{C}$; pulses of $0.5 \mu\text{l}$ EB, carrier gas flow rate 24 ml NTP/min). \times , Yields produced during a regular pulse sequence. \circ , Yield after $1/2$ h relaxation between two pulses. \otimes , Yields after 12 h relaxation.

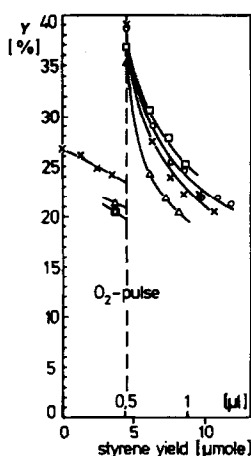


FIG. 16. Yield increases after pulsing of different amounts of oxygen. \square , $5 \times 500 \mu\text{l O}_2$. \circ , $3 \times 500 \mu\text{l O}_2$. \times , $1 \times 500 \mu\text{l O}_2$. Δ , $1 \times 250 \mu\text{l O}_2$.

styrene, which lies in the order of magnitude for estimates of the number of active centers (quinoid groups) on the surface of the coke (20).

The increase in activity of the catalyst for long pauses between two consecutive ethylbenzene injections, also in the absence of oxygen (cf. Fig. 15), may mean that oxygen bound within the bulk of carbon deposit is

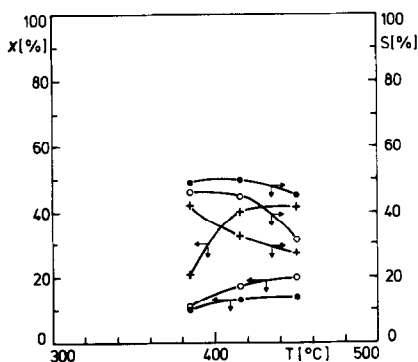


FIG. 17. Conversion and selectivity of ZrP-1 for butene oxydehydrogenation in an isothermal integral reactor as a function of temperature after more than 2 h on stream.

Butene/O₂/N₂

\bullet 1/0.5/6.2 } W/F = 3.0
 \circ 1/1.0/5.7 }
 $+$ 1/2.0/4.7 }

mobile and can diffuse to the active surface; alternatively some polystyrene polymer may depolymerize.

An oxygen pulse interspersed after a few ethylbenzene pulses immediately raises (depending on the amount of the oxygen pulsed) the degree of formation of styrene (Fig. 16).

(10) Another series of experiments in which butene-1 was dehydrogenated in a butene-oxygen mixture on zirconium phosphate ZrP-1 in an integral reactor is represented in Fig. 17. It shows a much lower activity and selectivity compared to ethylbenzene oxydehydrogenation (cf. Fig. 1), although some coke has been formed in these experiments, probably with a different structure. This suggests that an aromatic compound is needed for the formation of an active coke.

(11) If the quinoid structure functions as a redox system, the activity should be augmented by halogen substitutions on the basic aromatic ring (cf. quinone and tetrachloroquinone). For this reason ethylbenzene and oxygen were alternately pulsed in the pulse reactor, and at certain specified intervals a compound containing chlorine (HCl, CCl₄) was injected. Figure 18 shows that halogens do, indeed, augment the catalytic activity as expected. This could also explain the increase in selectivity referred to by Fujimoto *et al.* (24) during the formation of styrene on a Pd-KBr-Al₂O₃ catalyst where the coke which has been formed is

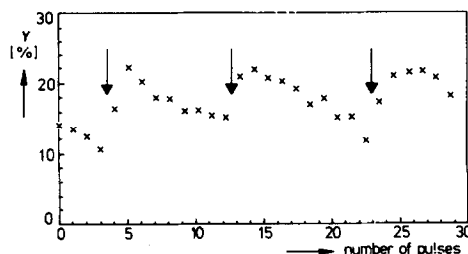


FIG. 18. Increase of styrene yield after pulses of chlorine-containing compounds ($T = 435^\circ\text{C}$; pulses of $15 \mu\text{l CCl}_4$ indicated by arrows, carrier gas flow rate 24 ml NTP/min).

partially halogenized, thus augmenting its dehydrogenation effect.

REFERENCES

1. British Pat. 999056, The Distillers Co. Ltd.
2. Offenlegungsschrift 1793433, BASF Ludwigshafen, 1971.
3. Auslegeschrift 1807666, The Badger Co., Cambridge, Mass., 1977.
4. U.S. Pat. 3502737, The Badger Co., Cambridge, Mass.
5. Alkhazov, T. G., *Kinet. Katal.* **13**, 509 (1972).
6. Rennard, R. J., *J. Catal.* **30**, 128 (1973).
7. U.S. Pat. 3733327, The Dow Chemical Co., 1973.
8. Iwasawa, J., Nobe, H., and Ogasawara, S., *J. Catal.* **31**, 444 (1973).
9. Cortes, A., and Seoane, J. L., *J. Catal.* **34**, 7 (1974).
10. Joseph, A., Mednick, R. L., Shorr, L. M., Weller, S. W., and Rona, P., *Israel J. Chem.* **12**(3), 739 (1974).
11. U.S. Pat. 3935126, The Dow Chemical Co., 1976.
12. Alkhazov, T. G., *Kinet. Katal.* **19**, 611 (1978).
13. Lisovskii, A. E., *Kinet. Katal.* **19**, 605 (1978).
14. Hattori, T., Hanai, H., and Murakami, Y., *J. Catal.* **56**, 294 (1979).
15. Degannes, P. N., and Ruthven, D. M., *Can. J. Chem. Eng.* **57**, 627 (1979).
16. Fiedorow, R., Przystajko, W., Sopa, M., and Dalla Lana, I. G., *J. Catal.* **68**, 33 (1981).
17. Murakami, Y., Iwayame, K., Uchida, H., Hattori, T., and Tagawa, T., *J. Catal.* **71**, 257 (1981); *Appl. Catal.* **2**, 67 (1982).
18. Batist, P. A., Lippens, B. C., and Schuit, G. C. A., *J. Catal.* **5**, 55 (1966).
19. Ruppert, W., Doctoral thesis, University of Erlangen-Nürnberg, 1981.
20. Trummer, L., Diploma thesis, University of Erlangen-Nürnberg, 1982.
21. Boehm, H. P., *Adv. Catal.* **16**, 179 (1966).
22. Papierer, E., Guyon, E., and Perol, N., *Carbon* **16**, 127 (1978).
23. Retcofsky, H. L., Hough, M. R., and Clarkson, R. B., *ACS Div. Fuel Chem. Prepr.* **24**(1), 83 (1979).
24. Fujimoto, K., and Kunugi, T., *Ind. Eng. Chem. Prod. Res. Dev.* **20**, 319 (1981).
25. Emig, G., and Hofmann, H., *Chem. Ztg.* **107**, 211 (1983).
26. Kürzinger, K., Doctoral thesis, University of Erlangen-Nürnberg, 1983.
27. Emig, G., and Hofmann, H., *J. Catal.* **8**, 303 (1967).
28. Benesi, A., and Winquist, B. H. C., *Adv. Catal.* **27**, 97 (1978).
29. Clearfield, A., and Smith, E. D., *Inorg. Chem.* **8**, 431 (1969).
30. Gasanova, N. I., Lisovski, A. E., Alkhazov, T. G., *Kinet. Katal.* **20**, 915 (1979).